Article

Cell Reports

# RONIN Is an Essential Transcriptional Regulator of Genes Required for Mitochondrial Function in the Developing Retina

## Graphical Abstract

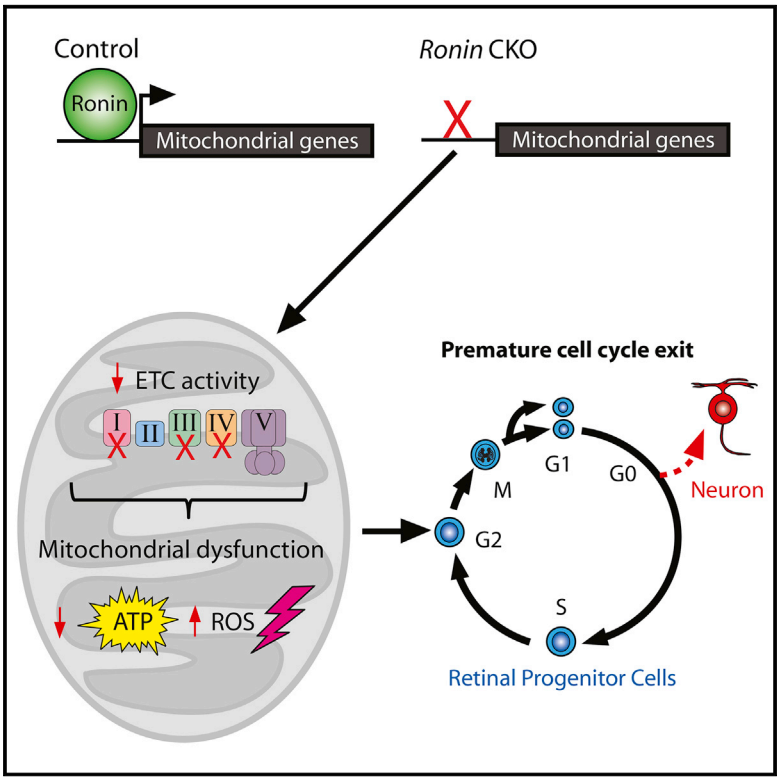


## Authors

Ross A. Poché, Min Zhang, Elda M. Rueda, ..., James F. Martin, Thomas P. Zwaka, Mary E. Dickinson

## Correspondence

poche@bcm.edu (R.A.P.), mdickins@bcm.edu (M.E.D.)

## In Brief

Poché et al. identify Ronin (Thap11) as an important regulator of mitochondrial gene expression that coordinates mitochondrial activity and cell-cycle progression. Loss of Ronin function leads to specific deficits in the electron transport chain as well as premature cell-cycle exit, excessive neurogenesis, and cell death.

## Highlights

- *Ronin* loss causes retinal progenitor cell-cycle arrest and photoreceptor degeneration
- Striking phenocopy of *Cyclin D1* nulls, but RONIN functions independently
- RONIN is a regulator of mitochondrial gene expression including ETC components
- RONIN coordinates mitochondrial activity and neural progenitor proliferation

## Accession Numbers

GSE74830

Poché et al., 2016, Cell Reports *14*, 1684–1697
February 23, 2016 ©2016 The Authors
http://dx.doi.org/10.1016/j.celrep.2016.01.039

OPEN ACCESS
CellPress

Cell Reports
Article

# RONIN Is an Essential Transcriptional Regulator of Genes Required for Mitochondrial Function in the Developing Retina

Ross A. Poché,[1,2,*] Min Zhang,[1] Elda M. Rueda,[6] Xuefei Tong,[1] Melissa L. McElwee,[1] Leeyean Wong,[1] Chih-Wei Hsu,[1] Marion Dejosez,[9,10] Alan R. Burns,[6] Donald A. Fox,[6,7,8] James F. Martin,[1,2,3,5] Thomas P. Zwaka,[9,10] and Mary E. Dickinson[1,2,3,4,*]

[1]Department of Molecular Physiology and Biophysics
[2]Program in Developmental Biology
[3]Cardiovascular Research Institute
Baylor College of Medicine, Houston, TX 77030, USA
[4]Department of Bioengineering, Rice University, Houston, TX 77005, USA
[5]Texas Heart Institute, Houston, TX 77030, USA
[6]College of Optometry
[7]Department of Biology and Biochemistry
[8]Department of Pharmacology
University of Houston, Houston, TX 77004, USA
[9]Department of Developmental and Regenerative Biology
[10]Black Family Stem Cell Institute
Icahn School of Medicine at Mount Sinai, New York, NY 10029, USA
*Correspondence: poche@bcm.edu (R.A.P.), mdickins@bcm.edu (M.E.D.)
http://dx.doi.org/10.1016/j.celrep.2016.01.039
This is an open access article under the CC BY-NC-ND license (http://creativecommons.org/licenses/by-nc-nd/4.0/).

## SUMMARY

**A fundamental principle governing organ size and function is the fine balance between cell proliferation and cell differentiation. Here, we identify RONIN (THAP11) as a key transcriptional regulator of retinal progenitor cell (RPC) proliferation. RPC-specific loss of *Ronin* results in a phenotype strikingly similar to that resulting from the G1- to S-phase arrest and photoreceptor degeneration observed in the *Cyclin D1* null mutants. However, we determined that, rather than regulating canonical cell-cycle genes, RONIN regulates a cohort of mitochondrial genes including components of the electron transport chain (ETC), which have been recently implicated as direct regulators of the cell cycle. Coincidentally, with premature cell-cycle exit, *Ronin* mutants exhibited deficient ETC activity, reduced ATP levels, and increased oxidative stress that we ascribe to specific loss of subunits within complexes I, III, and IV. These data implicate RONIN as a positive regulator of mitochondrial gene expression that coordinates mitochondrial activity and cell-cycle progression.**

## INTRODUCTION

The mammalian CNS is composed of an astonishing variety of morphologically and functionally distinct neuronal types organized with precise regional specification and connectivity. Throughout neurogenesis, cohorts of multi-potential neural progenitor cells exit the cell cycle and differentiate, gradually reducing the pool of proliferative progenitors over time. If too many progenitor cells prematurely exit the cell cycle and terminally differentiate, this depletes the progenitor pool for later differentiating neurons, resulting in hypoplasia and degeneration. Conversely, if neural progenitors fail to exit the cell cycle, hyperplasia, dysplasia, and tumor formation can result. Despite the strict requirement for coordinating progenitor proliferation with cell-cycle exit and differentiation in CNS development, the precise cellular and molecular mechanisms orchestrating these events are poorly understood.

The mouse retina is relatively simple in structure with only seven major cell types and is an excellent model system for studying mammalian CNS development. Retinogenesis begins at embryonic day 11 (E11.0) in a conserved, stereotypical order. Retinal ganglion cells (RGCs) emerge first, followed by temporally overlapping phases of horizontal, cone, amacrine, rod, bipolar, and Müller glial cell genesis (Sernagor, 2006; Young, 1985). Since all seven cell types are all derived from a common retinal progenitor cell (RPC) pool, the mouse retina is particularly well suited for studying how proliferation and differentiation are balanced so that all cell types are produced at the correct time and ratios for proper cytoarchitecture and visual processing. Despite advances in knowledge about transcriptional mechanisms driving RPC fate specification and differentiation, the manner in which RPC proliferation is regulated and coordinated with intrinsic fate specifying factors remains obscure. This is particularly true for transcriptional control of RPC proliferation.

Here, we examined the role of the embryonic stem cell (ESC) pluripotency factor RONIN (THAP11) during mouse

retinogenesis. RONIN was previously identified as a zinc-finger transcriptional regulator that is essential for ESC self-renewal and growth (Dejosez et al., 2008, 2010). Recently, several in vitro studies have alluded to an additional role as a direct regulator of cell proliferation (Parker et al., 2012, 2014). Therefore, we hypothesized that RONIN might play a role in balancing the proliferation of multipotent RPCs and neuronal differentiation. Using a conditional knockout (CKO) approach, we found that RONIN is indeed a key regulator of RPC proliferation. Specifically, CKO of *Ronin* in RPCs results in a striking phenocopy of the *Cyclin D1* null mutants in which RPCs undergo premature cell-cycle exit leading to a thin, hypoplastic adult retina (Das et al., 2009; Sicinski et al., 1995). Additionally, *Ronin* CKO retinae exhibit an unusual pattern of discontinuous photoreceptor degeneration that was previously described as a unique feature of the *Cyclin D1* mutants (Ma et al., 1998).

Based on emerging evidence that CYCLIN D1 acts as a retinal transcription factor (Bienvenu et al., 2010), we hypothesized that CYCLIN D1 and RONIN might function cooperatively in a transcription factor complex to directly control the expression of genes essential for regulating RPC proliferation, but we determined that *Ronin* and *Cyclin D1* do not interact at the genetic or protein level. Also, in contrast to recent in vitro reports (Parker et al., 2012, 2014), we did not identify enrichment of RONIN target genes within canonical cell-cycle pathways. Rather, we found that RONIN acts as a direct transcriptional regulator of nuclear-encoded mitochondrial genes. In particular and coincident with premature cell-cycle exit, *Ronin* CKO retinae suffer from a deficit in the electron transport chain (ETC) due to the de-regulation of genes that encode subunits of complex I, III, and IV. We also observed a reduction in ATP levels, oxidative stress, and the activation of mitochondrial quality-control pathways. This study identifies RONIN as a key transcription factor regulating both progenitor cell proliferation and mitochondrial activity during neural development.

## RESULTS

### *Ronin* Expression and RPC-Specific Knockout

qRT-PCR showed that *Ronin* transcripts were abundant in the E14.5 retina, decreasing by 2-fold by postnatal day 50 (P50) (Figure 1A). Similarly, immunofluorescence data showed a clear RONIN signal at E16.5 within the RPCs of the outer neuroblastic layer (onbl) and inner neuroblastic layer (inbl) with fainter signals within the ganglion cell layer (GCL) (Figure 1B). P20 retinae showed ubiquitous RONIN protein expression (Figure 1B). Analysis of a *Ronin-GFP* knockin allele showed ubiquitous expression of GFP (Figure 1C). These data suggested that Ronin might play a role in retinogenesis and possibly an additional role in mature retinal neurons.

Since germline loss of *Ronin* leads to preimplantation lethality (Dejosez et al., 2008), we generated *Chx10-Cre::GFP*$^{+/tg}$; *Ronin*$^{flox/flox}$ CKO mice in which *Ronin* loss occurs specifically within RPCs (Rowan and Cepko, 2004). CKO mice exhibited a dramatic reduction of *Ronin* transcripts at E14.5 compared to *Ronin*$^{flox/flox}$ controls (Figure 1D). Immunofluorescence at E16.5 further showed that RONIN protein was also lost within the CKO RPCs and their descendant neurons in the GCL (compare Figures 1B and 1E). We occasionally observed discrete patches of RONIN expression that persisted within the RPC population (arrow in Figure 1E) and visualization of CRE::GFP fluorescence indicated that these RONIN+ patches correspond to regions where *Chx10-Cre::GFP* is not expressed (arrowheads in Figure 1F). This finding suggests a low level of *Chx10-Cre::GFP* mosaicism, consistent with previous reports (Rowan and Cepko, 2004), and also confirms RONIN antibody specificity. Despite these occasional patches of residual RONIN expression, western blot analysis of *Ronin* CKO retinae confirmed that there was a general and dramatic decrease in RONIN protein beginning at E12.5 that became progressively more severe (Figure 1G).

### *Ronin* CKO Phenocopies the Adult *Cyclin D1* Null Mutants

*Ronin* CKO mice are viable, and analysis of the adult retinae revealed a striking structural phenotype. z stack confocal projections of DAPI-stained retinal flat mounts showed dramatic "holes" scattered throughout the photoreceptor layer in the CKO retinae that were not observed in controls (Figure 2A). This type of lesion was previously reported to be a unique feature of the *Cyclin D1* mutants, arising from localized photoreceptor degeneration (Ma et al., 1998), and the similarity was confirmed by direct comparison (Figure 2A). Both mutants had thin, hypoplastic retinae, suggesting a proliferation defect (Figure 2B), as well as inner nuclear layer (INL) cells infiltrating the degenerated outer nuclear layer (ONL) (Figure 2B, arrowheads). We also observed a striking *Cyclin D1* phenocopy at the level of RHODOPSIN loss near the degenerative lesions (Figure 2C, arrowheads) and corresponding GFAP+ reactive gliosis (Figure 2D) indicating that both *Ronin* and *Cyclin D1* mutants exhibit patchy retinal degeneration. Thus, *Ronin* loss within the embryonic retina impacts RPC proliferation and retinal neuron survival in a similar manner as *Cyclin D1* loss (Das et al., 2009; Sicinski et al., 1995). Consistent with these findings, CKO of *Ronin* broadly within the developing CNS recapitulated the ataxia and cerebellar hypoplasia described for the *Cyclin D1/D2* double mutants (Ciemerych et al., 2002) (Figure S1; Movies S1 and S2).

### *Ronin* Loss Results in Reduced RPC Proliferation and Premature Exit from the Cell Cycle

Quantification of the #EdU+/#DAPI+ pixels revealed a statistically significant decrease in S-phase entry as early as E14.5 and also at E18.5 (Figures 3A and 3B), that was also consistent with a reduction in KI67 immunofluorescence (Figure 3C). As another measure of *Ronin* CKO RPC proliferative capacity, we performed replication incompetent retroviral lineage analysis using either the NIN-E (control) or NIN-Cre (Cre-expressing) viruses, both of which encode a nuclear *LacZ* reporter and only infect proliferative RPCs (Dyer, 2003; Dyer and Cepko, 2001). Quantification of LacZ+ cells, examined 10 days following retinal explant and infection at E14.5 (Figure 3D), revealed that the NIN-Cre infected *Ronin*$^{flox/flox}$ retinae contained a significant increase in the percentage of single-cell clones and decrease in the percentage of clones that contained five or more cells as compared to the NIN-E infected retinae (Figure 3E). These data indicated that *Ronin* loss within RPCs directly contributes to premature

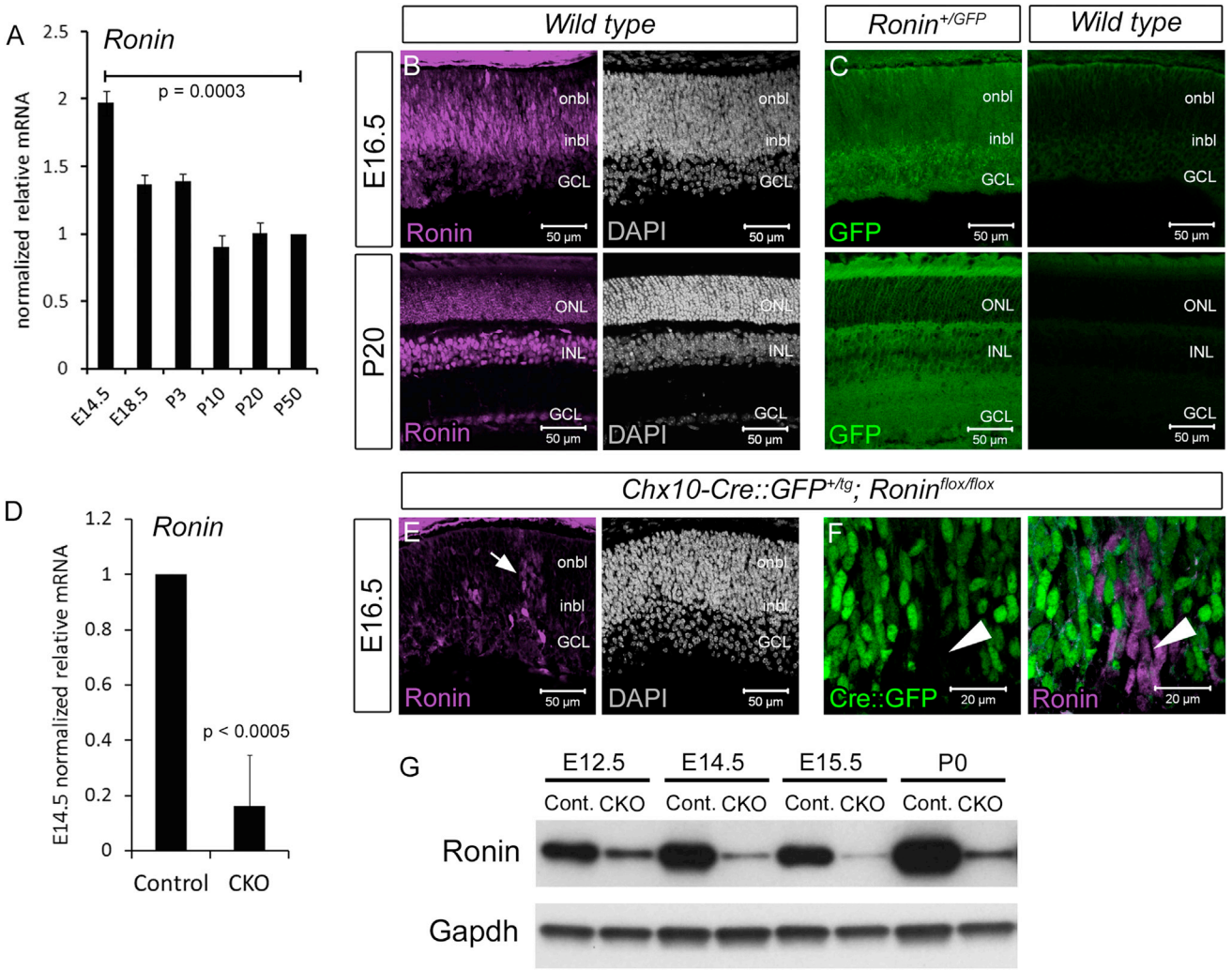


**Figure 1. *Ronin* Expression and Retinal-Specific Knockout**

(A) qRT-PCR time course of *Ronin* expression in the wild-type retina. Levels are given as relative to P50 (set to 1) and depicted as fold changes ± SEM (n = 3 independent pooled samples per time point; Student's t test).

(B) Ronin immunofluorescence in the E16.5 and P20 retina.

(C) Retinal GFP expression of *Ronin*$^{+/GFP}$ knockin allele.

(D) Reduction of *Ronin* mRNA expression in E14.5 RPC-specific CKOs. Levels are given as relative to control (set to 1) and depicted as fold change ± SEM (n = 3 independent pooled samples per group; Student's t test).

(E) Dramatic loss of Ronin protein within E16.5 RPCs. The arrow indicates an occasional patch of RPCs where Ronin expression persists.

(F) Ronin-positive patch corresponds to an area where Cre is not expressed.

(G) Western blot showing reduction of Ronin throughout retinogenesis.

cell-cycle exit in a cell-autonomous manner. However, we also detected a small but significant increase in activated CASPASE-3+ cells in the *Ronin* CKO retinae beginning at E16.5 (Figure S2A), further increasing by E18.5 and localized to the neuroblastic layer (NBL) and GCL (Figures S2A and S2B). Therefore, we cannot rule out the possibility that *Ronin* loss also triggers apoptosis that contributes to changes in mutant clone size. Additional analysis of apoptosis, using the *ROSA26R-mTmG*$^{+/tg}$ Cre reporter (Muzumdar et al., 2007) and RPC-specific markers, suggested that *Ronin* loss likely affects RPC and neuron survival in what is likely to be a cell-autonomous manner (Figure S2).

We also examined cell proliferation in *Ronin* retinal CKOs using the *Fucci* cell-cycle reporter mice, which label cells in the G1 phase with a red fluorescent protein and a GFP once cells enter the S phase and progress to G2 and M phase (Sakaue-Sawano et al., 2008). Post-mitotic retinal neurons also maintain red fluorescence (Sakaue-Sawano et al., 2008). We found that P0 *Ronin* CKO RPCs exhibited dramatically fewer cells in S, G2, and M phases, while the red fluorescence within the GCL appeared increased (Figure 3F). These results suggested that there are fewer proliferating RPCs in the *Ronin* CKOs and that premature exit from the cell cycle leads to overproduction

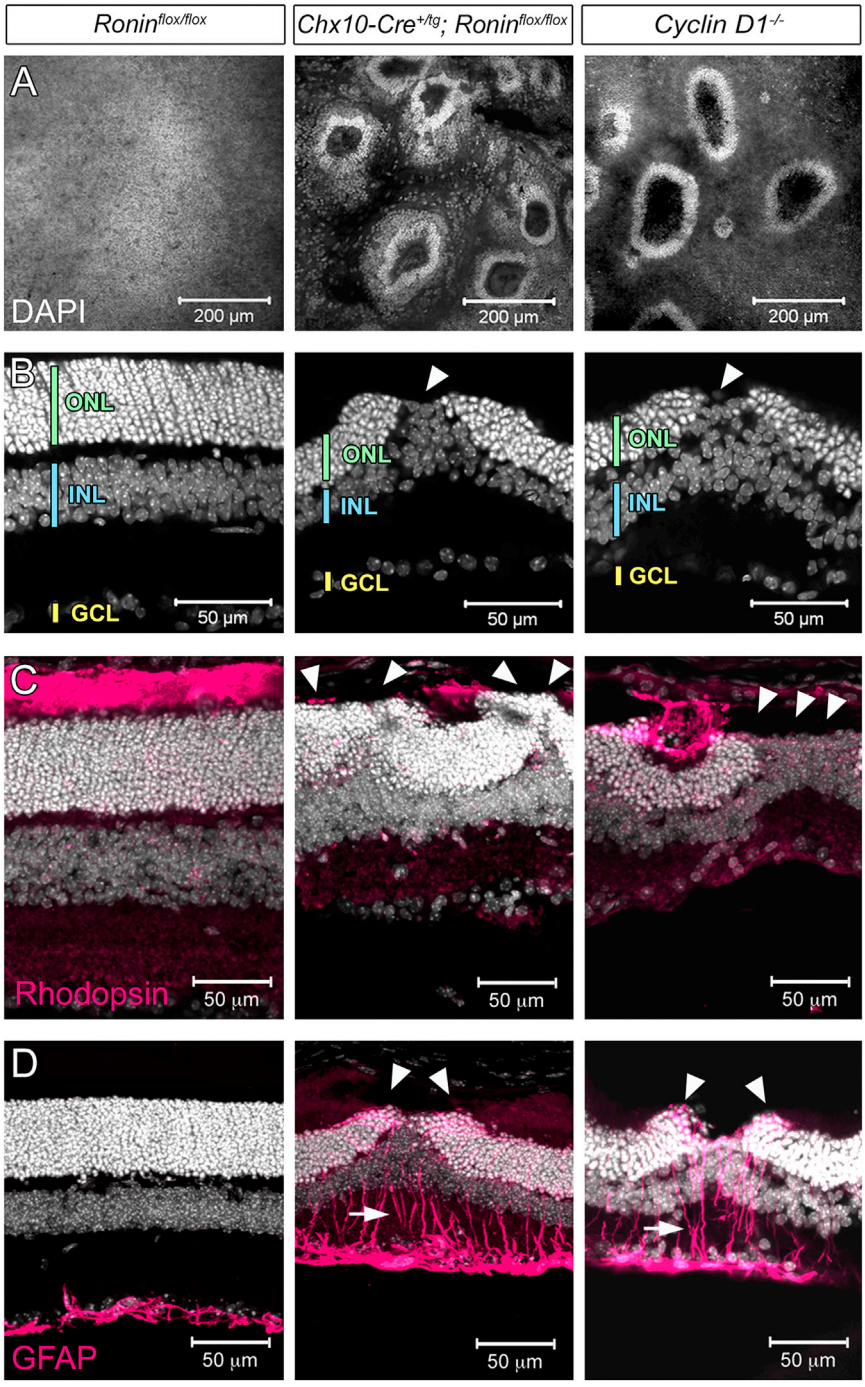


**Figure 2. Ronin CKOs Phenocopy the Cyclin D1$^{-/-}$ Retina**

(A) Retinal flat mounts stained with DAPI highlighting the holes scattered through out the *Ronin* and *Cyclin D1* mutants.

(B) Cryosections showing cross sections of the retinal holes (arrowheads) and thinning of the mutant retinae.

(C) Rhodopsin immunofluorescence showing loss within the mutant retinal lesions (arrowheads).

(D) GFAP immunofluorescence showing reactive gliosis (arrow) in the mutant retinae with astrocytes projecting into the retinal holes (arrowheads).

See also Figures S1 and S3.

of neurons. Consistent with this interpretation, E18.5 DAPI-stained sections showed that the RPC-containing NBL layer of the developing *Ronin* CKO retina was thinner than controls, while the post-mitotic, neuronal GCL appeared to be expanded (Figure 3G, green bars and red bars). We also observed a decrease in immunofluorescent labeling for the RPC-expressed transcription factor SOX2 (Figure 3G, white bars) (Taranova et al., 2006).

If the decrease in the *Ronin* mutant RPC population resulted from premature cell-cycle exit, as in the *Cyclin D1* mutants, we would expect to observe a consequential increase in the early retinal neuron population (Das et al., 2009). Using q-RT-PCR, we showed that the pro-neural gene *NeuroD1* was upregulated in both the *Ronin* CKO and *Cyclin D1* null E15.5 retinae, suggesting that both mutants exhibit excessive neurogenesis at the expense of the RPC pool (Figure 3H). NEUROD1 drives mouse retinogenesis and is transcriptionally upregulated in response to both *Notch1* and *Cyclin D1* loss (Hatakeyama and Kageyama, 2004; Yaron et al., 2006). Additionally, the domain of expression of pan-neuronal marker TUJ1 was also expanded in the *Ronin* CKO retinae at P0, coinciding with regions of CRE activity, again suggesting a cell-autonomous effect of *Ronin* loss (Figure 3I, arrows). Finally, we labeled E18.5 retinal flat mounts with antibodies against the RGC-specific marker BRN3B and imaged the GCL *en face* with confocal microscopy. We observed an increase in BRN3B+ RGCs within the E18.5 *Ronin* CKO retinae (Figures 3J and 3K). In total, these data support the conclusion that *Ronin* loss leads to premature exit of RPCs from the cell cycle resulting in excessive neuronal differentiation in a similar fashion to the *Cyclin D1* mutant retina.

## RONIN Is a Direct Transcriptional Regulator of Mitochondrial Gene Expression, Including Genes Required to Form ETC Complexes

Due to the similarities between the *Ronin* and *Cyclin D1* mutant retinae, and the recently established role for CYCLIN D1 as a

retinal transcription factor (Bienvenu et al., 2010), we reasoned that RONIN and CYCLIN D1 might functionally cooperate in a protein complex to regulate a specific cohort of genes that influence RPC proliferation. However, to our surprise, we found that RONIN and CYCLIN D1 do not interact genetically or at the protein level (Figure S3). Therefore, we hypothesized that RONIN-specific transcriptional targets are likely responsible for RPC cell-cycle arrest.

To identify these genes, we performed RONIN chromatin immunoprecipitation from P0 wild-type retinae followed by DNA sequencing (ChIP-seq). We found 904 RONIN-bound regions enriched within promoter regions throughout the genome, consistent with a role for RONIN as a transcriptional regulator (Figure 4A). Of these 904 RONIN ChIP-seq peaks, covering 898 genes, 305 also contained a conserved Ronin binding motif, which was previously identified in ESCs, and was enriched within promoter regions (Figure 4B). To focus our attention on the physiologically relevant ChIP-seq targets that are both expressed in RPCs and affected by *Ronin* loss, we performed RNA sequencing (RNA-seq) on E14.5 *Ronin* CKO and control retinae. This experiment revealed 124 genes that were upregulated and 247 that were downregulated in response to *Ronin* loss (Figure S4; Table S1). Overlay of these data with the ChIP-seq dataset revealed that 26 out of 124 upregulated genes and 99 out of 247 downregulated genes are bound by RONIN (Figures 4C and 4D; Tables S1 and S2), suggesting that RONIN functions as both a transcriptional repressor and activator during retinogenesis. Gene Ontology (GO) analysis of the overlapping ChIP-seq and RNA-seq data showed that the upregulated genes are involved in proteolysis, peptidase activity, and oxidation-reduction processes (Figure 4E; Table S3). Among the downregulated genes, we found enrichment for Ras GTPase binding, zinc ion binding, and mitochondrial genes (Figure 4F; Table S3). To our surprise, we did not detect significant enrichment of genes implicated in direct cell-cycle regulation or neurogenesis. Based on mounting evidence of the connection between mitochondrial activity and cell-cycle regulation (Lee and Finkel, 2013; Mandal et al., 2005; Mitra et al., 2009; Owusu-Ansah et al., 2008; Schieke et al., 2008; Wang et al., 2014), we chose to investigate the RONIN mitochondrial target genes in more detail.

Figure 5A shows a heatmap derived from the RNA-seq targets associated with the GO term "mitochondrion" that exhibited downregulation in the *Ronin* CKO retinae. Selected examples of the ChIP-seq peaks for a subset of these genes are shown in Figure 5B illustrating RONIN binding sites localized to promoter regions, and qRT-PCR analysis confirmed that these genes are downregulated in the *Ronin* CKOs (Figure 5C). Therefore, our ChIP-seq and RNA-seq screens identified genes expressed in the mitochondria of the developing retina that require RONIN activity for transcriptional activation. Mapping of mitochondrial-annotated RONIN ChIP-seq peaks to a schematic of a mitochondrion revealed that RONIN target genes are localized to different mitochondrial compartments and have various predicted functions (Figure 5D). However, we noticed two distinct clusters of genes with clearly defined roles in regulating ETC activity. One cluster (light blue box in Figure 5D) encodes subunits of ETC protein complexes I, III, IV, and V. The second cluster (dark purple box in Figure 5D) encodes three mitochondrial ribosomal proteins (MRPL24, MRPL34, and MRPL54) and the mitochondrial translational release factor (MTRF1). Since the 13 mitochondrial-encoded proteins are all core subunits of ETC complexes, the disruption of mitochondrial translation also negatively impacts ETC activity and results in a profound mitochondrial functional deficiency.

## *Ronin* CKO Retinae Show Signs of Oxidative Stress and Mitochondrial Damage

We next determined whether *Ronin* loss in the retina indeed results in compromised mitochondrial function and damage coincident with RPC cell-cycle arrest. First, we assessed general mitochondrial morphology within control and *Ronin* CKO P0 retinae by transmission electron microscopy (TEM). We noticed that the CKO retinal onbl contained what appeared to be swollen mitochondria with a loss of normal cristae morphology whereas control mitochondria had pronounced cristae (Figure 6A). However, TEM does not allow for the resolution of RPCs versus immature neurons. Furthermore, due to the low level Cre-mosaicism, we could not definitively identify *Ronin* CKO versus wild-type cells. Therefore, we performed additional histological assays as confirmation of mitochondrial dysfunction.

Freshly isolated retinal whole mounts were stained with the mitochondrial superoxide indicator MitoSOX, and we found that *Ronin* CKO retinae exhibited increased labeling within the onbl as compared to the negative controls (Figure 6B). By also imaging *Chx10-Cre::GFP* expression within the *Ronin* CKOs, we determined that the increase in MitoSOX labeling occurs in GFP-negative cells, suggesting that mitochondrial superoxides have accumulated predominantly within postmitotic cells versus RPCs. Consistent with this finding, immunofluorescence for the mitochondrial antioxidant manganese superoxide dismutase (MNSOD), which is a often increased during periods of oxidative stress (Dhar and St Clair, 2012), exhibited an increase within the CKO onbl, INL, and GCL at P0 as compared to controls (Figure 6C), and this was confirmed by western blot (Figure 6D). We next performed the OxyBlot assay and found that the *Ronin* CKO protein lysates had increased carbonylation, which is a hallmark of oxidative stress (Davies, 1987) (Figure 6E). Finally, we also noticed that *Parkin (Park2)* was one of the most upregulated transcripts in the *Ronin* CKO RNA-seq dataset, and qRT-PCR showed that its increase is almost 5-fold (Figures 6F and 6G). However, it is not enriched in our ChIP-seq data. Mutations in *PARK2* can cause Parkinson's disease and encode a protein that is essential for regulating mitochondrial quality control (Dagda and Chu, 2009; Shimura et al., 2000). Thus, its transcriptional upregulation is likely the consequence of mitochondrial dysfunction caused by *Ronin* loss.

## *Ronin* CKOs Exhibit a Specific Deficit in Mitochondrial ETC Activity

Previous work in *Drosophila* indicated that genetic ablation of specific ETC protein subunits drives a G1 to S phase cell-cycle arrest (Mandal et al., 2005; Owusu-Ansah et al., 2008). Of the RONIN ChIP-seq targets associated with the mitochondria, seven encoded proteins that are localized to the ETC complexes (Figure 7A) and all contained RONIN binding sites within their promoters (Figure 7B). To determine if ETC protein complex

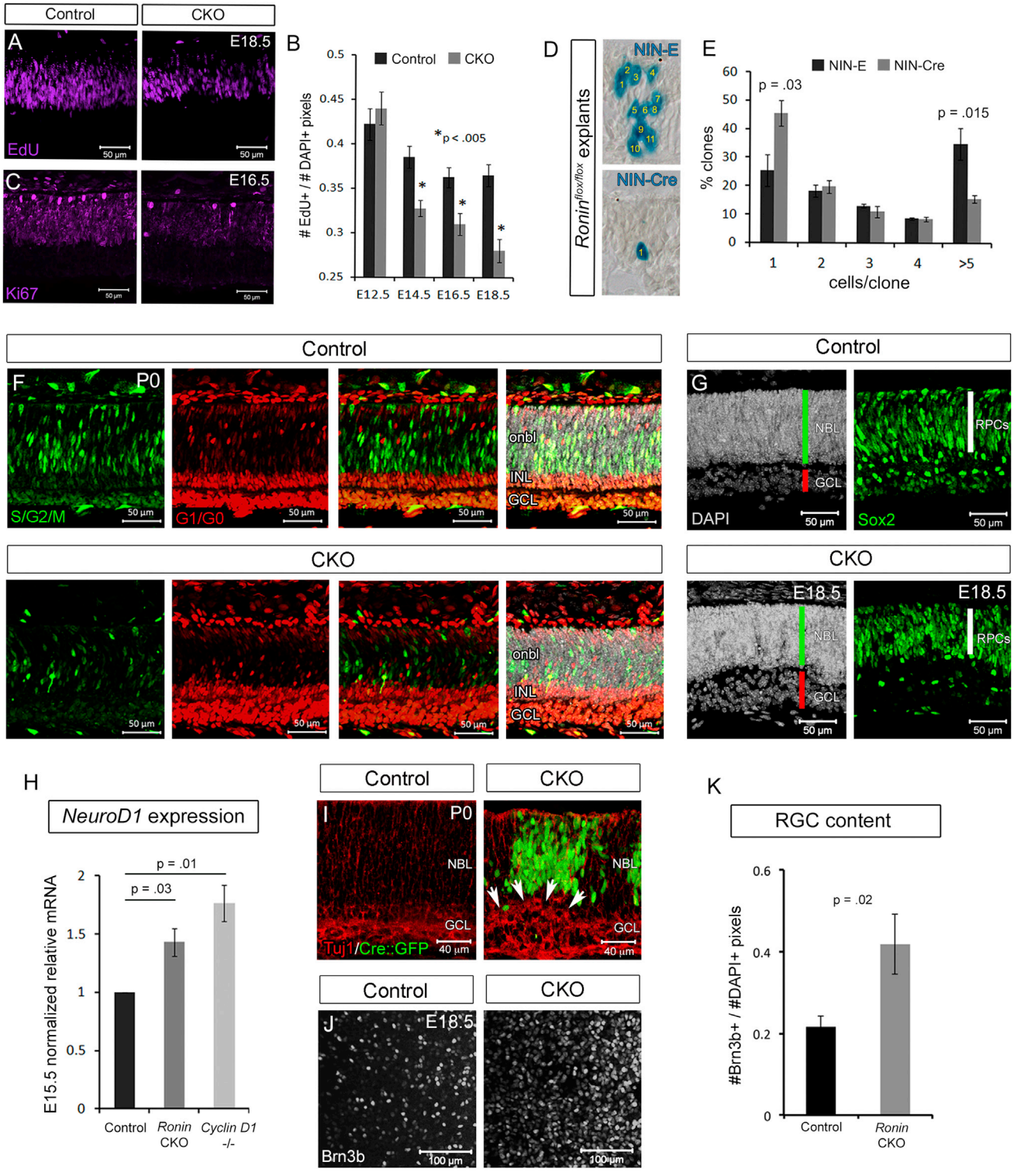


**Figure 3. Ronin Loss Results in Premature Cell-Cycle Exit and Excessive Neurogenesis**

(A and B) EdU labeling of *Ronin* CKO retinae represented as the average ratio ± SEM of EdU-positive pixels to DAPI-positive pixels (n = 3 samples per group; Student's t test).

(C) CKOs show a reduction in immunofluorescence for Ki67.

(D) Representative images of nuclear LacZ-labeled control (NIN-E) and *Ronin* mutant (NIN-Cre) clones.

*(legend continued on next page)*

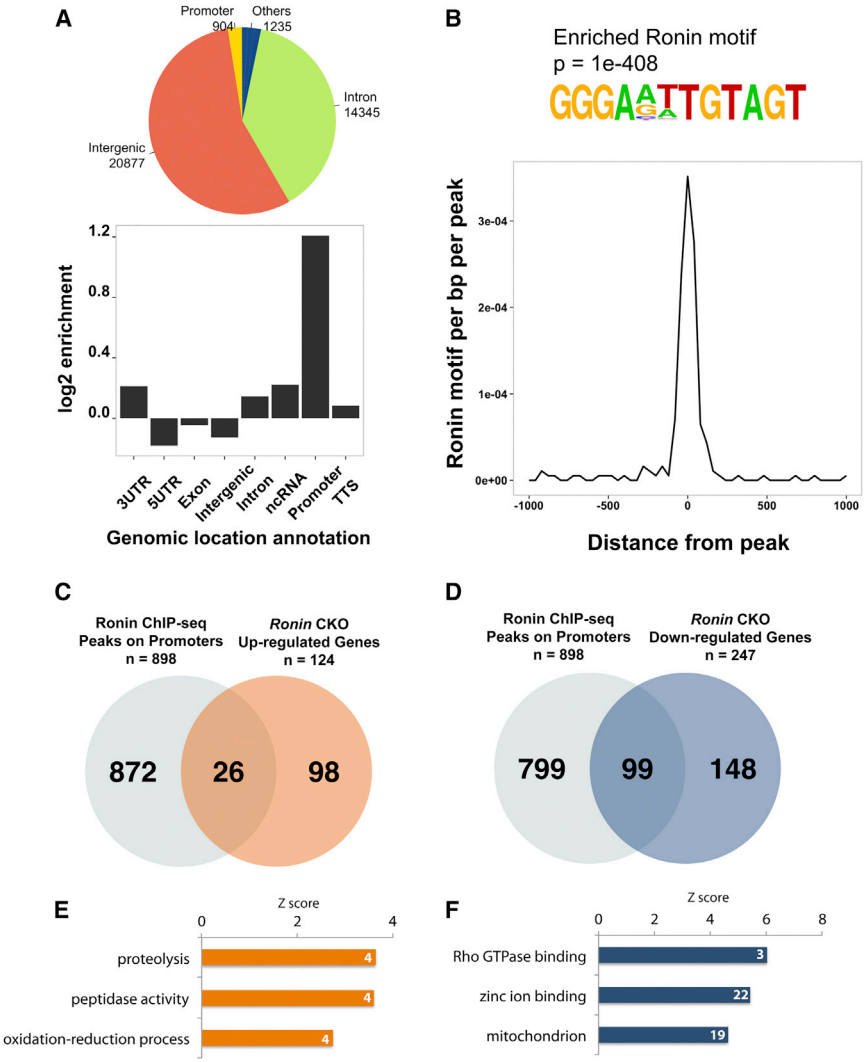


**Figure 4. ChIP-Seq and RNA-Seq Analyses**

(A) Distribution of Ronin binding sites throughout the P0 retinal genome and significant enrichment at promoter regions.

(B) Enrichment of a known Ronin binding motif within ChIP-seq peaks.

(C and D) Overlap of ChIP-seq with E14.5 *Ronin* CKO RNA-seq data showing upregulation (C) and downregulation (D).

(E and F) Gene Ontology (GO) analysis of the genes upregulated and downregulated in the ChIP-seq/RNA-seq overlap that showed a significant *Z* score. The numbers inside the bars correspond to the number of genes within the overlapping datasets that associate with that particular GO term.

See also Figure S4.

formation requires *Ronin*, we performed qRT-PCR on *Ronin* CKO and control retinae and found that *Ndufa3*, *Uqcr10*, and *Cox7c* were transcriptionally downregulated. These genes encode protein components of ETC complex I, III, and IV, respectively. Interestingly, *Ndufv1*, *Atp5d*, and *Atp5o* showed slight increases in mRNA levels, suggesting that they are possibly negatively regulated by RONIN or upregulated via a compensatory mechanism responding to an ETC deficiency (Figure 7C).

ETC complexes are large, multi-subunit complexes and have been shown to exhibit reductions in stability and/or formation when complex subunits are missing and when partner complexes within ETC supercomplexes are disrupted (Acin-Perez and Enriquez, 2014; Acín-Pérez et al., 2008). We investigated whether the reduction in *Ndufa3*, *Uqcr10*, and *Cox7c* mRNA levels observed in the *Ronin* CKO retinae impact the presence of ETC protein complexes. Western blot analysis showed both E15.5 and P0 *Ronin* CKO retinae exhibited a significant reduction in NDUFA9, UQCRC2, and COX4 proteins corresponding to complex I, III, and IV, respectively. However, complex II protein SDHA and complex V protein ATP5A were unaffected (Figure 7D). We further confirmed this finding by using an independent set of ETC antibodies and found that NDUFB8, UQCRC1, and COX1 proteins were all dramatically reduced, again suggesting disruption of complex I, III, and IV. SDHB and ATP5B levels were unchanged, providing additional evidence that complex II and V are not affected (Figure 7E). Importantly, we did not detect any changes in levels of non-ETC mitochondrial proteins VDAC1 or POLG (Figure 7F). We also crossed the *mito-Dendra2* mitochondrial fluorescent transgene reporter into the *Ronin* CKOs, and we did not observe any changes in mito-Dendra2 protein levels (Figure 7G) (Pham et al., 2012). Taken together, these data suggest that *Ronin* loss does not generally impact mitochondrial content. Rather,

(E) Scoring of clone composition is represented as the average percentage of clones ± SEM of a specific size (n = 4 samples per group; Student's t test).

(F) Labeling of cell-cycle phases with the Fucci transgenes shows a decrease in cells within S/G2/M-phase.

(G) *Ronin* CKOs exhibit a diminishment of the Sox2+ RPC population.

(H) E15.5 *Ronin* and *Cyclin D1* mutants have increased NeuroD1 mRNA expression. Levels are given as relative to independent littermate controls (set to 1) and depicted as fold changes ± SEM (n = 3 independent pooled samples per group; Student's t test).

(I) The domain of pan-neuronal marker Tuj1 expression is expanded in the *Ronin* CKOs.

(J and K) Ronin CKOs contain more Brn3b+ RGCs represented as the average ratio ± SEM of Brn3b-positive pixels to DAPI-positive pixels (n = 3 samples per group; Student's t test).

See also Figures S2 and S3.

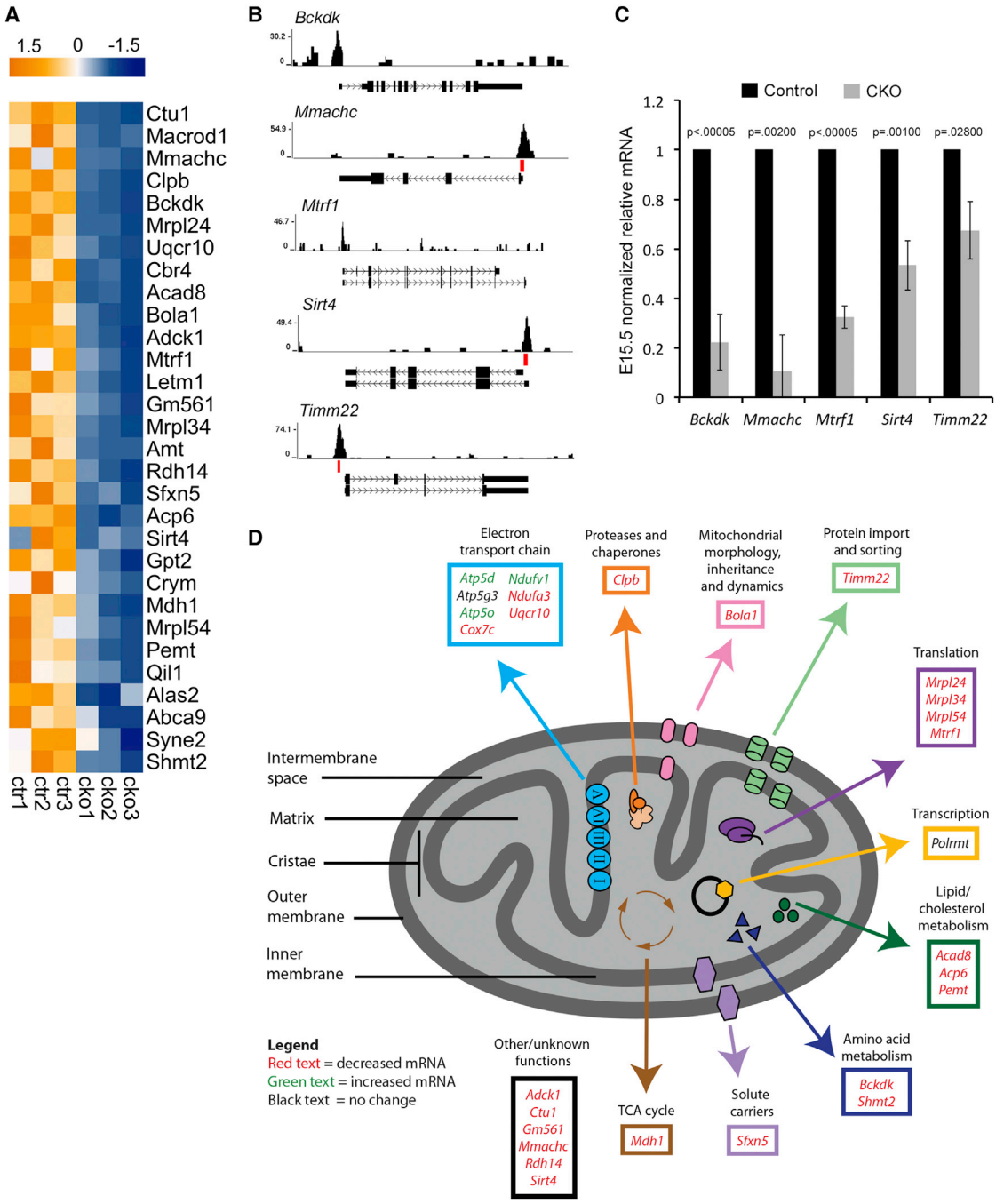


**Figure 5. Ronin Regulates a Diverse Cohort of Mitochondrial Genes**

(A) Heatmap from *Ronin* CKO RNA-seq showing 30 mitochondrial genes that are downregulated (fold change $\geq$ 1.5, FDR $\leq$ 0.2).

(B) Images of Ronin ChIP-seq peaks within promoter regions shown for a subset of the genes in the RNA-seq heatmap. The red boxes denote the presence of a Ronin binding motif.

(C) E15.5 qRT-PCR analysis of *Ronin* CKO retinae confirming a reduction in mRNA expression of representative ChIP-seq targets. Levels are given as relative to the control (set to 1) and depicted as fold changes ± SEM (n = 3 independent pooled samples per group; Student's t test).

(D) Genes with a Ronin ChIP-seq peak specifically within the promoter region that also show transcriptional downregulation either by RNA-seq, qRT-PCR or both (red), upregulation by qRT-PCR (green), or no change by RNA-seq and qRT-PCR (black) were mapped to a schematic of a mitochondrion and functionally annotated.

the mRNA reduction we observed at the level of the Ronin target genes *Ndufa3*, *Uqcrc10*, and *Cox7c* likely impacts the stability and/or formation of ETC complexes I, III, and IV.

As a functional assessment of ETC, we performed cytochrome *c* oxidase (COX) histochemistry on E15.5 and P0 retinal cryosections. Despite the findings that the *mito-Dendra2* transgene clearly showed mitochondria present in neurons within the P0 *Ronin* CKOs GCL and inner plexiform layer (IPL) (Figure 7H, arrow) and that the mtDNA content was actually increased (Figure 7I), we uncovered a dramatic reduction in COX activity, which was obvious as early as E15.5 and became progressively more severe by P0 (compare Figures 7J–JL). This result shows that a transcriptional reduction in key ETC RONIN target genes ultimately results in a deficiency in complex IV activity in vivo. Consistent with the ETC deficit, we showed that P0 *Ronin* CKO retinae exhibited a significant (almost 50%) reduction in ATP levels relative to controls (Figure 7M). Thus, taken together, these data strongly implicate Ronin as a major regulator of ETC activity in the developing retina.

## DISCUSSION

We have uncovered a role for RONIN (THAP11) as a transcriptional regulator that profoundly influences RPC proliferation and retinal neuron survival. By conditionally knocking out *Ronin*, we showed that the balance of RPC proliferation and differentiation is disrupted as RPCs prematurely exit the cell cycle and the retina experiences excessive embryonic neurogenesis and apoptosis. Ultimately, this results in a thin, underdeveloped adult tissue that also phenocopies the discontinuous pattern of photoreceptor degeneration previously described as a unique feature of the *Cyclin D1* mutant mice (Ma et al., 1998). However, molecular and genetic interaction experiments revealed that RONIN functions independently of CYCLIN D1. To our surprise, ChIP-seq and RNA-seq experiments identified a cohort of nuclear-encoded mitochondrial genes that are bound by RONIN and are significantly reduced in *Ronin* CKO retinae. Seven of these target genes encode ETC complex subunits and are directly required for ETC function, which has been directly implicated in cell-cycle G1 to S phase regulation (Mandal et al., 2005; Owusu-Ansah et al., 2008). Our data indicate that dysregulation of mitochondrial function following *Ronin* loss has a significant impact on the normal proliferation, differentiation, and survival of retinal progenitor cells.

Our studies also revealed a large group of zinc ion binding genes enriched in our Ronin retinal ChIP-seq and RNA-seq datasets. However, none of these factors have been clearly implicated in cell-cycle regulation, mitochondrial activity, or retinogenesis. Future efforts will be aimed at clarifying their roles in the retina.

### RONIN as a Major Regulator of Mitochondrial Gene Expression and Activity

In our analyses of the *Ronin* CKO retinae, we observed distinct signs of mitochondrial oxidative stress and the activation of quality-control pathways, which we attribute to loss of nuclear-encoded RONIN target genes necessary for proper mitochondrial function. Our finding that RONIN plays such a profound role in regulating the expression of proteins required for mitochondrial biogenesis and function is significant, because only a handful of such nuclear-encoded transcription factors have been identified, including PGC-1$\alpha$, NRF-1, NRF-2, and TFAM (Scarpulla et al., 2012; Wu et al., 1999). Therefore, our data raise the obvious question of whether RONIN functionally interacts with these factors. Interestingly, the zebrafish mutant for *not really finished* (*nrf*), the homolog of mammalian *Nrf-1*, was shown to exhibit a thin, underdeveloped retina with patchy, degenerative lesions reminiscent of the *Ronin* and *Cyclin D1* mutants (Becker et al., 1998). In *Drosophila*, Cyclin D is a positive regulator of mitochondrial function by influencing the activity of *nrf-1* and its target gene, *tfam* (Icreverzi et al., 2012; Icreverzi et al., 2015). However, there are also contradictory data suggesting that mammalian CYCLIN D1 is actually a negative regulator of NRF-1 activity, inhibiting mitochondrial biogenesis (Sakamaki et al., 2006; Wang et al., 2006). Based on the co-immunoprecipitation results presented here, we do not believe that there is a direct protein/protein interaction between RONIN and CYCLIN D1, and we have P0 retinal immunoprecipitation data suggesting that interactions between NRF-1 and RONIN or its co-factor, HCF1, do not occur (Figure S5). Thus, our understanding of the interactions between mitochondrial transcription factors is far from complete, and future studies should be focused on identifying additional RONIN co-factors.

### A Role for RONIN in Regulating RPC Proliferation and Retinal Neuron Survival

RONIN has been identified as a transcriptional regulator that influences ESC pluripotency and growth, but a role in regulating proliferation and/or differentiation during neural development in vivo has not been described (Dejosez et al., 2008, 2010). However, a recent in vitro study has suggested an additional role for RONIN in transcriptional regulation of the cell cycle (Parker et al., 2014). HeLa cells were shown to contain a RONIN/HCF-1/ZNF143 transcription factor complex that is enriched on E2F-bound promoters of genes implicated in cell proliferation. While these genes are represented in our RONIN ChIP-seq dataset and we cannot conclusively rule them out as contributing to the *Ronin* CKO retinal phenotype, only one of these genes (*Bod1*) was significantly reduced within our RNA-seq dataset. Furthermore, we have not been able to detect the presence of ZNF143 protein in RONIN and HCF1 co-immunoprecipitations from P0 mouse retinal lysates (data not shown). It is also important to note that while the *E2f1/2/3* triple-mutant retinae have increased RPC apoptosis, unlike *Ronin* CKOs, it is specifically restricted to the P0 time point. Additionally, these mice have a modest proliferation defect, and there is no report of the discontinuous pattern of photoreceptor degeneration observed in the *Ronin* and *Cyclin D1* mutants (Chen et al., 2009).

Based on our finding that RONIN is an important transcriptional regulator ETC components and other mitochondrial genes, we propose that RONIN impacts RPC proliferation and retinal neuron survival at the level of mitochondrial activity rather than cell-cycle gene expression. This idea is consistent with several groundbreaking studies in *Drosophila* that implicated ETC complex I and III in directly influencing the G1 to S phase transition (Mandal et al., 2005; Owusu-Ansah et al., 2008). Specifically,

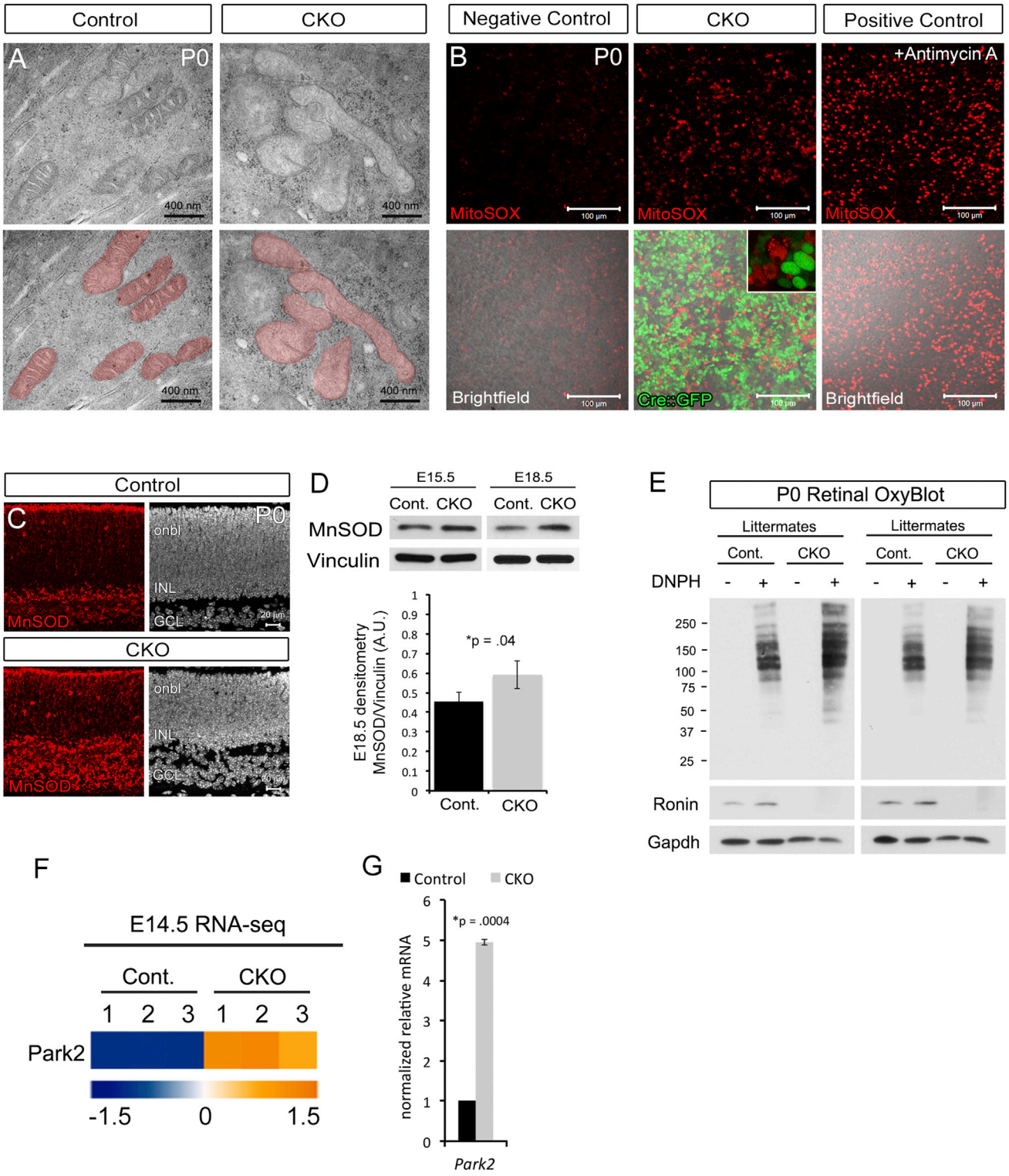


**Figure 6. Ronin CKO Retinae Exhibit Signs of Oxidative Stress**

(A) TEM image of control and *Ronin* CKO P0 retinae.

(B) MitoSOX Red staining and Cre::GFP expression in P0 *Ronin*$^{flox/flox}$ (negative control), *Ronin* CKOs, and *Ronin*$^{flox/flox}$ treated with Antimycin A (positive control) retinal whole mounts imaged at the level of the onbl.

(C) MnSOD immunofluorescence indicated an increase within the P0 *Ronin* CKO INL and GCL.

*(legend continued on next page)*

we found that *Ronin* CKO retinae showed a reduction in ETC protein complex I, III, and IV assembly and/or stability coincident with premature exit from the RPC cell cycle. We attribute this to a decrease in expression of RONIN target genes *Ndufa3*, *Uqcr10*, and *Cox7c,* whose gene products reside in these complexes. It is especially interesting that we observed reductions in ETC complex I, III, and IV, as these are known to form a functionally interdependent supercomplex called the respirasome. Upon disruption of one of these complexes, the partners within the supercomplex are affected and overall activity is compromised (Acín-Pérez et al., 2008; Moreno-Lastres et al., 2012; Schäfer et al., 2006). This is also reflected in our finding that *Ronin* CKO retinal COX activity and ATP levels are reduced.

## RONIN and CYCLIN D1 Function Likely Converge upon Mitochondrial Activity

Given the remarkable phenocopy between *Ronin* and *Cyclin D1* mutant retinae and cerebella, we were surprised that we did not detect either a genetic or molecular interaction. CYCLIN D1 recently emerged as a protein of immense functional diversity with roles not only within the canonical cell-cycle pathway but also in transcriptional regulation, DNA repair, glucose metabolism, and apoptosis (Bienvenu et al., 2010; Choi et al., 2014; Jirawatnotai et al., 2011, 2012; Lee et al., 2014). Therefore, there may be aspects of CYCLIN D1 function, possibly relating to RONIN, that remain to be discovered. We favor the hypothesis that RONIN and CYCLIN D1 play independent roles and the commonality they share is at the level of regulating mitochondrial activity. Furthermore, the unusual pattern of photoreceptor degeneration observed in both the *Ronin* CKO and the *Cyclin D1* null retinae (Ma et al., 1998) might result from aberrant mitochondrial function.

In the case of RONIN, we presented integrative and multidisciplinary results that support its role as a transcriptional regulator of mitochondrial gene expression that, when lost, compromises the ETC and likely other mitochondrial functions. It is possible that CYCLIN D1 might also regulate mitochondrial gene expression, albeit via a separate cohort from those regulated by RONIN. It is also conceivable that CYCLIN D1 might influence mitochondrial function at the protein level. Recent CYCLIN D1 mass spectrometry data suggest possible interactions with mitochondrial proteins (Bienvenu et al., 2010). Even more tantalizing is a recent report that CYCLIN B1 and associated CDKs physically transport to the mitochondria to phosphorylate ETC components, which increases ATP production in preparation for M phase (Wang et al., 2014). CYCLIN D1 might play a similar role as CYCLIN B1, but at the G1 to S phase transition. While there is still much to be learned about the role mitochondria play in directly regulating the cell cycle, our study identifies RONIN as a transcriptional regulator of mitochondrial gene expression with significant impact on future investigations of the transcriptional networks coordinating mitochondrial activity with neural progenitor cell proliferation and terminal differentiation.

## EXPERIMENTAL PROCEDURES

See Supplemental Experimental Procedures for detailed protocols, lists of reagents, statistics, and associated references.

### Mouse Strains

The following mouse lines were used and PCR genotyped using published protocols: *Ronin*$^{flox/flox}$, *Ronin*$^{+/GFP}$, *Chx10Cre::GFP*$^{+/tg}$, *Fucci*, *Gfap-Cre*$^{+/tg}$, *ROSA26R-mTmG*$^{+/tg}$, *Cyclin D1*$^{-/-}$, *p27Kip1*$^{-/-}$, and *Mito-Dendra*$^{+/tg}$. All animal research was conducted according to protocols approved by the Institutional Animal Care and Use Committee of Baylor College of Medicine.

### Histology and Microscopy

Immunofluorescence, X-gal staining, and confocal microscopy of cryosections were performed as previously described with minor modifications (Poché et al., 2007). COX histochemistry was performed as previously described (Wong-Riley, 1979). To label retinal progenitors in S phase, 5-ethynyl-2′-deoxyuridine (EdU) was injected intraperitoneally (IP) into pregnant dams at a concentration of 50 mg/kg body weight. After 2 hr, mice were sacrificed to harvest embryos for retinal cryosections and EdU detection with the Click-iT Plus EdU Alexa Fluor 555 Kit (ThermoFisher). For TEM, posterior eyecups were fixed in cold 3% paraformaldehyde + 3% glutaraldehyde in 0.1 M sodium cacodylate for 2 days, post-fixed in 1% $OsO_4$, dehydrated in an EtOH series, and embedded in Epon. 80- to 90-nm sections were cut and stained with uranyl acetate and lead citrate. To detect mitochondrial superoxide, freshly dissected retinae were incubated with 5 μm MitoSOX Red (Molecular Probes, #M36008), diluted in 1× PBS, for 10 min at 37°C followed by gentle washing in 1× PBS at 37°C. As a positive control, *Ronin*$^{flox/flox}$ retinae were treated with 5 μM of the ETC complex III inhibitor antimycin A for 1 hr at 37°C prior to staining.

### RNA Isolation, qRT-PCR, and RNA-Seq

Retinae were dissected and total RNA immediately purified using the RNeasy Mini Kit (QIAGEN) followed by reverse transcription using the SuperScript III first-strand synthesis kit (Invitrogen). The TaqMan gene expression assay from Applied Biosystems was used to assess differences between control and mutant retinae. For RNA-seq, total RNA was poly-A selected and fractionated (200–500 nt range). cDNA was generated using the Invitrogen SuperScript III reverse transcription kit followed by second-strand cDNA synthesis and then subjected to standard Illumina adaptor ligation and sequencing. Alignment of RNA-seq data were performed using the bwa (version 0.7.6a) analysis pipeline against mouse genome mm9. Significant differences were called using cutoffs p value $\leq$ 0.05, fold change $\geq$ 1.5, and false discovery rate (FDR) $\leq$ 0.10.

### Protein Isolation, Western Blot, Oxyblot, and Immunoprecipitation

Retinae were homogenized in Pierce lysis buffer (Thermo Fisher Scientific, #87787) supplemented with Halt protease inhibitor cocktail (Thermo Fisher, #78430). Protein was then run on 4%–15% Tris-HCl precast gels (Bio-Rad, #3450027) and transferred (30 V, overnight) onto Immobilon-P PVDF Membranes (Millipore) using the Criterion system (Bio-Rad). Blots from at least 3 independent controls and *Ronin* CKOs were incubated with primary antibodies (in 5% milk, overnight at 4°C) followed by incubation with horseradish-peroxidase-conjugated secondary antibodies, detection with ECL Substrate (Thermo Fisher, #32106), and exposure to film (Phenix, F-BX57). The OxyBlot protein oxidation detection kit (EMD Millipore, #S7150) was used following the

(D) Western blot of E15.5 and E18.5 *Ronin* CKO confirmed a slight increase in MnSOD protein at E15.5 and a significant increase by E18.5.
(E) Independent Oxyblot assays of P0 retinal lysates showed that *Ronin* CKO retinae undergo excessive protein oxidation.
(F) Heat map from the *Ronin* CKO RNA-seq showing the increase in *Park2* (fold change $\geq$ 1.5, FDR $\leq$ 0.2).
(G) qRT-PCR confirmation that the *Park2* mRNA level is increased in the *Ronin* CKOs. Levels are given as relative to the control (set to 1) and depicted as fold change ± SEM (n = 3 independent pooled samples per group; Student's t test).

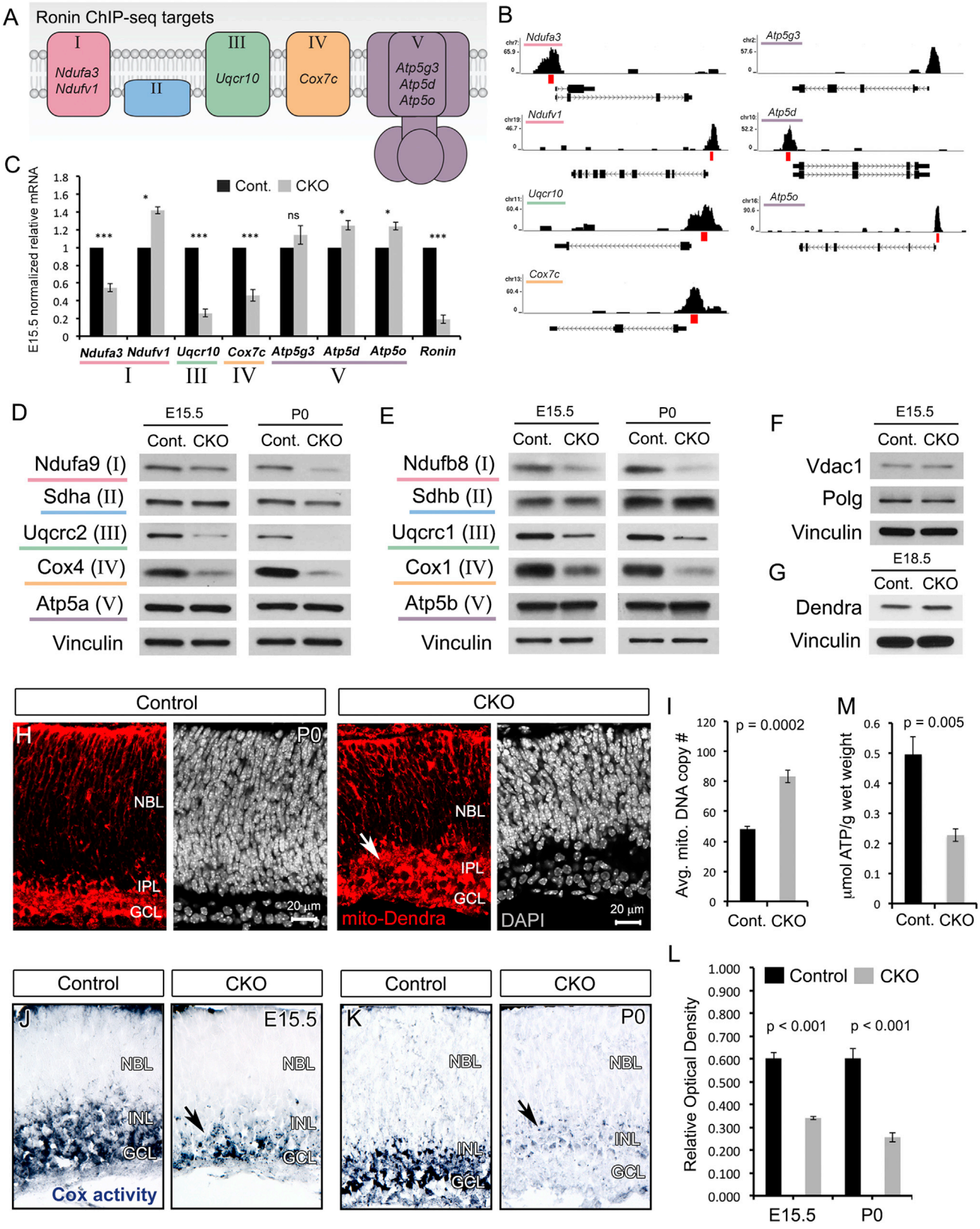


*(legend on next page)*

manufacturer's instructions. For details on co-immunoprecipitation experiments, please see Supplemental Experimental Procedures.

### ChIP, ChIP-qPCR, and ChIP-Seq

Chromatin immunoprecipitation was performed as described previously (Mao et al., 2013). For ChIP-qPCR, to assess whether RONIN binds intron 2 of *Notch1*, purified RONIN-bound DNA was amplified using SYBR Green PCR master mix (ThermoFisher, #4309155). ChIP libraries were created and sequenced using the Ion Torrent PGM system. Reads were mapped to the mm9 assembly (NCBI Build 37) using Torrent Suite (2.0.1) aligner Tmap (0.2.3) (Life Technologies). The cutoffs for calling the peaks were read-number enriched at least 4-fold, with an FDR threshold of 0.001, FDR effective Poisson p value of 1.3e-6, and minimum read number of 6.

## ACCESSION NUMBERS

The accession number for the RNA-seq and ChIP-seq data (Edgar et al., 2002) reported in this paper is GEO: GSE74830 (http://www.ncbi.nlm.nih.gov/geo/query/acc.cgi?acc=GSE74830).

## SUPPLEMENTAL INFORMATION

Supplemental Information includes Supplemental Experimental Procedures, five figures, three tables, and two movies and can be found with this article online at http://dx.doi.org/10.1016/j.celrep.2016.01.039.

## AUTHOR CONTRIBUTIONS

Conceptualization, R.A.P., and M.E.D.; Methodology, R.A.P., M.E.D., T.P.Z., M.D., and J.F.M.; Formal Analysis, R.A.P., M.Z., and J.F.M.; Investigation, R.A.P., M.Z., E.M.R., X.T., M.L.M., L.W., and C.W.; Writing – Original Draft, R.A.P.; Writing – Reviews and Editing, R.A.P. and M.E.D.; Resources, A.R.B., M.D., D.A.F., J.F.M., and T.P.Z; Funding Acquisition, R.A.P., M.E.D., and J.F.M.

## ACKNOWLEDGMENTS

We thank E. Levine for providing the *Cyclin D1* null mice and M. Dyer for NIN-E and NIN-Cre plasmids. We thank the Vector Development Lab (BCM) for purifying the NIN-E and NIN-Cre retroviruses and the Genomics Core Facility at the Icahn School of Medicine for assistance with RNA-seq. We thank B. Reese, J. Jankowsky, A. Groves, J. Culver, and M. Dyer for critical reading of the manuscript. This work was supported by grants from the NIH (R01 EY024906 to R.A.P.; R01 EB016629 and P20 EB007076 to M.E.D.; R01 DE023177 and R01 HL118761 to J.F.M.; and P30 EY002520 and P30 EY007551), the Kyle and Josephine Morrow Endowed Chair (M.E.D.), the Vivian L. Smith Foundation (J.F.M.), and the Knights Templar Eye Foundation Career Starter Grant (R.A.P.).

Received: November 12, 2015
Revised: December 14, 2015
Accepted: January 10, 2016
Published: February 11, 2016

## REFERENCES

Acin-Perez, R., and Enriquez, J.A. (2014). The function of the respiratory supercomplexes: the plasticity model. Biochim. Biophys. Acta *1837*, 444–450.

Acín-Pérez, R., Fernández-Silva, P., Peleato, M.L., Pérez-Martos, A., and Enriquez, J.A. (2008). Respiratory active mitochondrial supercomplexes. Mol. Cell *32*, 529–539.

Becker, T.S., Burgess, S.M., Amsterdam, A.H., Allende, M.L., and Hopkins, N. (1998). not really finished is crucial for development of the zebrafish outer retina and encodes a transcription factor highly homologous to human Nuclear Respiratory Factor-1 and avian Initiation Binding Repressor. Development *125*, 4369–4378.

Bienvenu, F., Jirawatnotai, S., Elias, J.E., Meyer, C.A., Mizeracka, K., Marson, A., Frampton, G.M., Cole, M.F., Odom, D.T., Odajima, J., et al. (2010). Transcriptional role of cyclin D1 in development revealed by a genetic-proteomic screen. Nature *463*, 374–378.

Chen, D., Pacal, M., Wenzel, P., Knoepfler, P.S., Leone, G., and Bremner, R. (2009). Division and apoptosis of E2f-deficient retinal progenitors. Nature *462*, 925–929.

Choi, Y.J., Saez, B., Anders, L., Hydbring, P., Stefano, J., Bacon, N.A., Cook, C., Kalaszczynska, I., Signoretti, S., Young, R.A., et al. (2014). D-cyclins repress apoptosis in hematopoietic cells by controlling death receptor Fas and its ligand FasL. Dev. Cell *30*, 255–267.

Ciemerych, M.A., Kenney, A.M., Sicinska, E., Kalaszczynska, I., Bronson, R.T., Rowitch, D.H., Gardner, H., and Sicinski, P. (2002). Development of mice expressing a single D-type cyclin. Genes Dev. *16*, 3277–3289.

Dagda, R.K., and Chu, C.T. (2009). Mitochondrial quality control: insights on how Parkinson's disease related genes PINK1, parkin, and Omi/HtrA2 interact to maintain mitochondrial homeostasis. J. Bioenerg. Biomembr. *41*, 473–479.

Das, G., Choi, Y., Sicinski, P., and Levine, E.M. (2009). Cyclin D1 fine-tunes the neurogenic output of embryonic retinal progenitor cells. Neural Dev. *4*, 15.

Davies, K.J. (1987). Protein damage and degradation by oxygen radicals. I. general aspects. J. Biol. Chem. *262*, 9895–9901.

Dejosez, M., Krumenacker, J.S., Zitur, L.J., Passeri, M., Chu, L.F., Songyang, Z., Thomson, J.A., and Zwaka, T.P. (2008). Ronin is essential for embryogenesis and the pluripotency of mouse embryonic stem cells. Cell *133*, 1162–1174.

Dejosez, M., Levine, S.S., Frampton, G.M., Whyte, W.A., Stratton, S.A., Barton, M.C., Gunaratne, P.H., Young, R.A., and Zwaka, T.P. (2010). Ronin/Hcf-1 binds to a hyperconserved enhancer element and regulates genes involved in the growth of embryonic stem cells. Genes Dev. *24*, 1479–1484.

**Figure 7. Ronin Loss Results in a Functional Deficit in the ETC**

(A) Schematic of the ETC highlighting genes that contain Ronin ChIP-seq peaks.
(B) ChIP-seq peaks within ETC genes. The red boxes denote the presence of a Ronin binding motif.
(C) qRT-PCR analysis of ETC target genes showing changes in mRNA levels. Levels are given as relative to the control (set to 1) and depicted as fold changes ± SEM (n = 3 independent pooled samples per group; Student's t test). ***$p < 0.0005$ and *$p < 0.01$.
(D) Western blot of protein subunits within the ETC showing a decrease in complex I, III, and IV in the CKOs.
(E) Independent set of antibodies confirming the finding in (D).
(F and G) Levels of the non-ETC mitochondrial proteins Vdac1 and Polg (F) and the mitochondrial-targeted Dendra protein (from the mito-Dendra transgene) (G) are unaffected by *Ronin* loss.
(H) *Ronin* CKO and control mice expressing mito-Dendra show that the *Ronin* CKO mitochondrial content is not reduced (arrow).
(I) The *Ronin* CKO mtDNA content is increased relative to controls. Levels are given as the average number of copies of mtDNA ± SEM (n = 3 independent pooled samples per group; Student's t test).
(J–L) Cytochrome *c* oxidase (COX) histochemistry of E15.5 and P0 *Ronin* CKOs revealed a dramatic decrease in COX activity. Levels were given as average optical density values ± SEM (n > 3 independent samples per group; Student's t test).
(M) *Ronin* CKOs have reduced ATP levels represented as the average micromoles ATP per wet weight ± SEM (n = 3 independent pooled samples per group; Student's t test).

Dhar, S.K., and St Clair, D.K. (2012). Manganese superoxide dismutase regulation and cancer. Free Radic. Biol. Med. *52*, 2209–2222.

Dyer, M.A. (2003). Regulation of proliferation, cell fate specification and differentiation by the homeodomain proteins Prox1, Six3, and Chx10 in the developing retina. Cell Cycle *2*, 350–357.

Dyer, M.A., and Cepko, C.L. (2001). p27Kip1 and p57Kip2 regulate proliferation in distinct retinal progenitor cell populations. J. Neurosci. *21*, 4259–4271.

Edgar, R., Domrachev, M., and Lash, A.E. (2002). Gene Expression Omnibus: NCBI gene expression and hybridization array data repository. Nucleic Acids Res. *30*, 207–210.

Hatakeyama, J., and Kageyama, R. (2004). Retinal cell fate determination and bHLH factors. Semin. Cell Dev. Biol. *15*, 83–89.

Icreverzi, A., de la Cruz, A.F., Van Voorhies, W.A., and Edgar, B.A. (2012). Drosophila cyclin D/Cdk4 regulates mitochondrial biogenesis and aging and sensitizes animals to hypoxic stress. Cell Cycle *11*, 554–568.

Icreverzi, A., de la Cruz, A.F., Walker, D.W., and Edgar, B.A. (2015). Changes in neuronal CycD/Cdk4 activity affect aging, neurodegeneration, and oxidative stress. Aging Cell *14*, 896–906.

Jirawatnotai, S., Hu, Y., Michowski, W., Elias, J.E., Becks, L., Bienvenu, F., Zagozdzon, A., Goswami, T., Wang, Y.E., Clark, A.B., et al. (2011). A function for cyclin D1 in DNA repair uncovered by protein interactome analyses in human cancers. Nature *474*, 230–234.

Jirawatnotai, S., Hu, Y., Livingston, D.M., and Sicinski, P. (2012). Proteomic identification of a direct role for cyclin d1 in DNA damage repair. Cancer Res. *72*, 4289–4293.

Lee, I.H., and Finkel, T. (2013). Metabolic regulation of the cell cycle. Curr. Opin. Cell Biol. *25*, 724–729.

Lee, Y., Dominy, J.E., Choi, Y.J., Jurczak, M., Tolliday, N., Camporez, J.P., Chim, H., Lim, J.H., Ruan, H.B., Yang, X., et al. (2014). Cyclin D1-Cdk4 controls glucose metabolism independently of cell cycle progression. Nature *510*, 547–551.

Ma, C., Papermaster, D., and Cepko, C.L. (1998). A unique pattern of photoreceptor degeneration in cyclin D1 mutant mice. Proc. Natl. Acad. Sci. USA *95*, 9938–9943.

Mandal, S., Guptan, P., Owusu-Ansah, E., and Banerjee, U. (2005). Mitochondrial regulation of cell cycle progression during development as revealed by the tenured mutation in Drosophila. Dev. Cell *9*, 843–854.

Mao, C.A., Cho, J.H., Wang, J., Gao, Z., Pan, P., Tsai, W.W., Frishman, L.J., and Klein, W.H. (2013). Reprogramming amacrine and photoreceptor progenitors into retinal ganglion cells by replacing Neurod1 with Atoh7. Development *140*, 541–551.

Mitra, K., Wunder, C., Roysam, B., Lin, G., and Lippincott-Schwartz, J. (2009). A hyperfused mitochondrial state achieved at G1-S regulates cyclin E buildup and entry into S phase. Proc. Natl. Acad. Sci. USA *106*, 11960–11965.

Moreno-Lastres, D., Fontanesi, F., García-Consuegra, I., Martín, M.A., Arenas, J., Barrientos, A., and Ugalde, C. (2012). Mitochondrial complex I plays an essential role in human respirasome assembly. Cell Metab. *15*, 324–335.

Muzumdar, M.D., Tasic, B., Miyamichi, K., Li, L., and Luo, L. (2007). A global double-fluorescent Cre reporter mouse. Genesis *45*, 593–605.

Owusu-Ansah, E., Yavari, A., Mandal, S., and Banerjee, U. (2008). Distinct mitochondrial retrograde signals control the G1-S cell cycle checkpoint. Nat. Genet. *40*, 356–361.

Parker, J.B., Palchaudhuri, S., Yin, H., Wei, J., and Chakravarti, D. (2012). A transcriptional regulatory role of the THAP11-HCF-1 complex in colon cancer cell function. Mol. Cell. Biol. *32*, 1654–1670.

Parker, J.B., Yin, H., Vinckevicius, A., and Chakravarti, D. (2014). Host cell factor-1 recruitment to E2F-bound and cell-cycle-control genes is mediated by THAP11 and ZNF143. Cell Rep. *9*, 967–982.

Pham, A.H., McCaffery, J.M., and Chan, D.C. (2012). Mouse lines with photoactivatable mitochondria to study mitochondrial dynamics. Genesis *50*, 833–843.

Poché, R.A., Kwan, K.M., Raven, M.A., Furuta, Y., Reese, B.E., and Behringer, R.R. (2007). Lim1 is essential for the correct laminar positioning of retinal horizontal cells. J. Neurosci. *27*, 14099–14107.

Rowan, S., and Cepko, C.L. (2004). Genetic analysis of the homeodomain transcription factor Chx10 in the retina using a novel multifunctional BAC transgenic mouse reporter. Dev. Biol. *271*, 388–402.

Sakamaki, T., Casimiro, M.C., Ju, X., Quong, A.A., Katiyar, S., Liu, M., Jiao, X., Li, A., Zhang, X., Lu, Y., et al. (2006). Cyclin D1 determines mitochondrial function in vivo. Mol. Cell. Biol. *26*, 5449–5469.

Sakaue-Sawano, A., Kurokawa, H., Morimura, T., Hanyu, A., Hama, H., Osawa, H., Kashiwagi, S., Fukami, K., Miyata, T., Miyoshi, H., et al. (2008). Visualizing spatiotemporal dynamics of multicellular cell-cycle progression. Cell *132*, 487–498.

Scarpulla, R.C., Vega, R.B., and Kelly, D.P. (2012). Transcriptional integration of mitochondrial biogenesis. Trends Endocrinol. Metab. *23*, 459–466.

Schäfer, E., Seelert, H., Reifschneider, N.H., Krause, F., Dencher, N.A., and Vonck, J. (2006). Architecture of active mammalian respiratory chain supercomplexes. J. Biol. Chem. *281*, 15370–15375.

Schieke, S.M., McCoy, J.P., Jr., and Finkel, T. (2008). Coordination of mitochondrial bioenergetics with G1 phase cell cycle progression. Cell Cycle *7*, 1782–1787.

Sernagor, E. (2006). Retinal Development (Cambridge University Press).

Shimura, H., Hattori, N., Kubo, Si., Mizuno, Y., Asakawa, S., Minoshima, S., Shimizu, N., Iwai, K., Chiba, T., Tanaka, K., and Suzuki, T. (2000). Familial Parkinson disease gene product, parkin, is a ubiquitin-protein ligase. Nat. Genet. *25*, 302–305.

Sicinski, P., Donaher, J.L., Parker, S.B., Li, T., Fazeli, A., Gardner, H., Haslam, S.Z., Bronson, R.T., Elledge, S.J., and Weinberg, R.A. (1995). Cyclin D1 provides a link between development and oncogenesis in the retina and breast. Cell *82*, 621–630.

Taranova, O.V., Magness, S.T., Fagan, B.M., Wu, Y., Surzenko, N., Hutton, S.R., and Pevny, L.H. (2006). SOX2 is a dose-dependent regulator of retinal neural progenitor competence. Genes Dev. *20*, 1187–1202.

Wang, C., Li, Z., Lu, Y., Du, R., Katiyar, S., Yang, J., Fu, M., Leader, J.E., Quong, A., Novikoff, P.M., and Pestell, R.G. (2006). Cyclin D1 repression of nuclear respiratory factor 1 integrates nuclear DNA synthesis and mitochondrial function. Proc. Natl. Acad. Sci. USA *103*, 11567–11572.

Wang, Z., Fan, M., Candas, D., Zhang, T.Q., Qin, L., Eldridge, A., Wachsmann-Hogiu, S., Ahmed, K.M., Chromy, B.A., Nantajit, D., et al. (2014). Cyclin B1/Cdk1 coordinates mitochondrial respiration for cell-cycle G2/M progression. Dev. Cell *29*, 217–232.

Wong-Riley, M. (1979). Changes in the visual system of monocularly sutured or enucleated cats demonstrable with cytochrome oxidase histochemistry. Brain Res. *171*, 11–28.

Wu, Z., Puigserver, P., Andersson, U., Zhang, C., Adelmant, G., Mootha, V., Troy, A., Cinti, S., Lowell, B., Scarpulla, R.C., and Spiegelman, B.M. (1999). Mechanisms controlling mitochondrial biogenesis and respiration through the thermogenic coactivator PGC-1. Cell *98*, 115–124.

Yaron, O., Farhy, C., Marquardt, T., Applebury, M., and Ashery-Padan, R. (2006). Notch1 functions to suppress cone-photoreceptor fate specification in the developing mouse retina. Development *133*, 1367–1378.

Young, R.W. (1985). Cell differentiation in the retina of the mouse. Anat. Rec. *212*, 199–205.